

PHOTO RESTORATION USING MULTIREOLUTION TEXTURE SYNTHESIS AND CONVOLUTIONAL NETWORKS

Gunturu Pradeep Chandra¹, K. Rajasekhar²

¹Department of Electronics and Communication Engineering, University College of Engineering, Kakinada, India

²Assistant Professor, Department of Electronics and Communication Engineering, University College of Engineering, Kakinada

Abstract - Digital cameras and mobile phones allow us to record valuable moments conveniently. While digital picture quality is continually improving, taking high-quality photographs of digital screens continues difficult as the photographs are often contaminated with moiré patterns due to interference between camera sensor pixel grids and computer screen. Moiré patterns can include dots, stripes, lines, haze, fog, and so on. There were few studies aimed at solving the problem of removing haze and fog conditions, but some did not get the highest signal to noise ratio and SSIM. Our technique achieves the elimination of haze and fog circumstances with the largest signal-to-noise ratio by using the IDeRS algorithm where the dehazing process can be performed and the image restoration can be completely solved.

Key Words: Moiré pattern, image restoration, texture synthesis, Denoising, Dehazing Process, IDeRS.

1. Introduction:

Now a days, digital cameras and mobile phones play a significant role in people's lives. They enable us to capture precious moments that are interesting and meaningful. While capturing the pictures, due to the mobiles or some external factors some artifacts are formed on the image. The artifacts which are formed on the image is known as Moiré Pattern. The moiré pattern may be consists of dots, lines, some irrelevant patterns, haze and also fog.

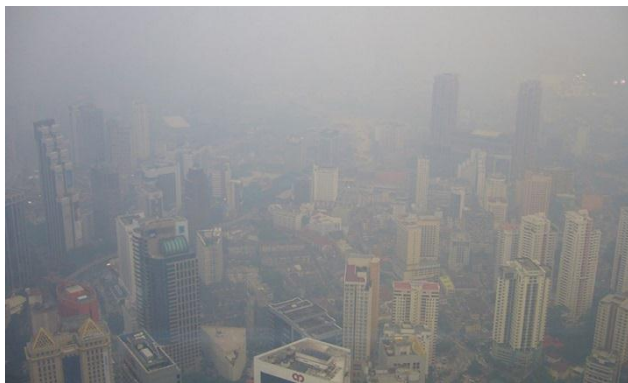


Figure 1: A hazy image with fog consisting of buildings.

Not only the mobile phone cameras captured photos contains haze and fog but also the surveillance cameras captured photos also contains noise substances like haze and fog. Due to the above reasons, "hazes" of RSI are those translucent covering-contaminations covering on the earth's surface, such as haze/fog, thin cloud, snow, silt, dust, off gas, etc. To enhance the quality of RSI, RSI improvement has been extensively studied, However, the enhancement ignored the physical mechanism of haze so that it cannot remove haze perfectly, generally suffering from over-saturation and gradient reversal artifacts. In fact, haze increases exponentially along with the optical distances from scene objects to the sensor for RSIs.

Firstly, the natural image is captured by the camera pointing to the distance, where image contrast and colour saturation get worse and worse along with the increase of scene depth. This property gives a variety of priors [5] for deriving transmission map for NID. However, RSI is usually captured by remote optical sensors aboard satellite far from the earth, so its scene depth is equally a constant.

Secondly, the atmospheric light, with few exceptions, is often estimated in an ad-hoc manner [6] or decided by the most haze opaque pixel [7]. The haze-opaque region mostly refers sky region in natural image. Moreover, there is usually no sky region in a RSI.

Thirdly, RSIs are often captured in a wide variety of spatial resolution, scale and shape of the objects on the earth's surface, whereas natural images are mostly with the similar resolution and scale. Accordingly, the hazes have variety in RSIs. So, NID methods designed for a simple image cannot effectively remove the hazes of RSIs. These three differences compromise the efficiency of a NID as it is applied to RSID.

Recently, learning based dehazing has been developed in a large manner [8]. It is trained on a database of image pairs of clean image and hazy image. In the database, hazy images are generated from computer models which require accurate scene depth measurement, which is however not attainable up to now for outdoor scenes, including RSIs. Considering above three differences, we propose an Iterative Dehazing model for Remote Sensing image (IDeRS).

2. Haze physical model:

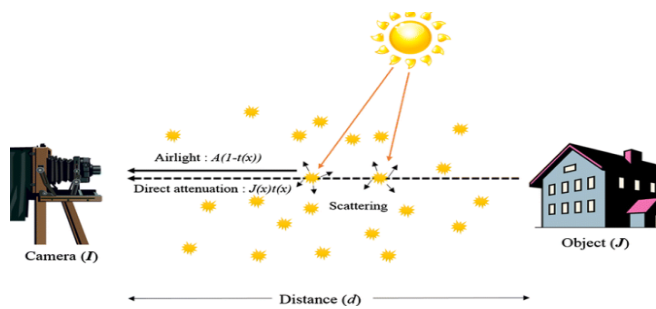


Figure 2: Formation of a Hazy image.

2.1 Haze image physical model:

The physical model for NID is described as

$$I(x) = J(x) \cdot t(x) + A (1 - t(x)), \quad (1)$$

Where I is the hazy picture and x represents the spatial coordinates, J is the radiance of the scene. A is the atmospheric light, i.e. at infinite distance light intensity (known as the haze opaque region), which is commonly assumed as the global constant. $t(x) \in [0,1]$ is the transmission map depicting the light part can reach the camera without dispersed.

2.2 Haze physical model for natural image:

Visibility restoration [1] discusses about different methods that aim to reduce or remove the degradation that have occurred while the digital image was being obtained. The image quality [2] of outdoor screen in the fog and haze weather condition is generally degraded by the scattering of a light before reaching the camera due to these large quantities of suspended particles (e.g. haze, smoke, fog, impurities) in the atmosphere.

Haze is usually an atmospheric phenomenon where dust, smoke and other dry particles obscure the transparency of the sky. Haze formation is thought as a phenomenon of dry air, mist formation is a phenomenon of humid air. When sunlight come across tiny pollution particles in the air, haze is formed. Some light is absorbed by the particles. Other light is scattered before it touches an observer. More impurities in the air indicates more absorption and scattering of light, which reduce the clarity and color of what we see.

2.2.1 Phone Model Specifications:

Manufacturer	Model	Camera
APPLE	iPhone 8	12MP
SAMSUNG	Galaxy S8	12MP

SONY	Xperia Z5	23MP
MOTOROLA	Moto one	13MP

Table 1: Some of the Mobile phone specifications for capturing the pictures.

2.2.2 Display Screen Specifications:

Manufacturer	Model	Resolution	Size (inch)
APPLE	Mac book Pro Retina	2500*1600	13.3"
DELL	U2410 LCD	1920*1200	24"
HP	Pavilion	1920*1080	14"

Table 2: Some of the Display Screen specifications for viewing the image.

A natural image is captured on the ground where the camera points at the distance. It usually contains haze-opaque region (commonly, the sky region). Then the atmospheric light A can be computed from the brightest pixel, or a portion of the brightest pixels. A RSI is captured by the camera aboard satellite where the camera points downward the ground, so it commonly has no haze-opaque region. The bright pixels commonly belong to the reflect light of objects' surface, which cannot be used to calculate atmospheric light A . Hence, A estimation should be independent of haze-opaque for RSID. After evaluating the state-of-the-arts, including the DCP, colour-line prior, blind dehazing, DehazeNet and haze-line prior, the haze-line prior is finally selected to estimate A in this work. Haze-line prior claims that pixels' intensities of objects with similar colours form lines in RGB space under haze. These lines intersect at the atmospheric light colour. Using Hough transform, where the point with the highest vote is assumed to be the atmospheric light colour.

We now have a uniform model for both natural image and RSI. Hence, the computation of transmission map for RSI is still being employed by the conventional DCP mode. The term "virtual depth" is interpreted in brief as following: the objects on the earth's surface have different surface reflectance coefficients or surface albedos, so they commonly show different colour saturations in a RSI. Low saturation may be caused by the objects with light colour. In this sense, "virtual depth" denotes the translucent covering of the earth's surface, which has the same effect of scene depth in a natural image.

2.3 Dehazing for Remote Sensing image:

Dehazing is important in remote sensing image restorations to enhance the acquired low quality image for interpretation. However, traditional methods have some

limitations for dehazing of remote sensing images due to its colour distortion and noise. Based on the discussion about transmission map estimation and atmospheric light estimation, the IDeRS are presented in detail.

2.3.1 Estimation of raw transmission map by using DCP:

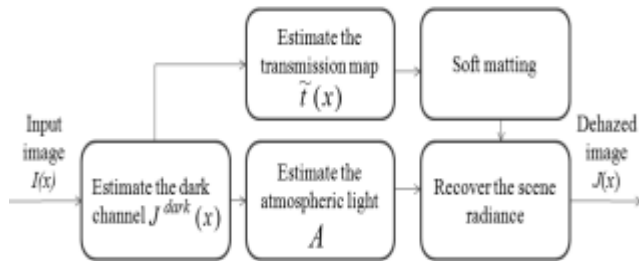


Figure 3: The Flowchart of DCP Scheme

Note that in the DCP system the dark channel is discovered by the 15×15 window minimum filtering and the transmission is acquired by the dark channel. The dark channel with a minimum 15×15 filter makes its ms in the neighborhood mixed with portion of the picture, particularly in the region of big discontinuities of depth. Therefore, if the transmission $t(x)$ is not refined, a severe halo issue occurs. In the DCP scheme, the soft matting algorithm was used to refine $t(x)$ which results in the problem of high computation cost. In the raw transmission map was estimated by $t(x) = 1 - \min_{y \in \Omega(x)} [\min_{c \in \{r,g,b\}} I_c(y) / A_c]$, where I_c and J_c is a hazy image colour channel I and haze-free scene radiance J , respectively. $\Omega(x)$ is a local patch at x . A_c is given by A_r, A_g or A_b for colour image. From, $t(x)$ is a local path constant Ω , which may cause block artifact surrounding patches. Therefore, Guided Image Filter (GIF) can be used for further compressing block artifact. The result is denoted by $tgif$, and the method is cited by GDCP. On the other side, we discover a clue to prevent smooth matting when looking at transmission maps with distinct window dimensions. It is noted that there is no need for refinement and therefore no halo issue either, if the minimum 1×1 filter is used to estimate the dark channel. In other words, the halo issue arises from the dark channel discovered through the 15×15 window minimum filter.

When using 1 built-in window, the transmission map does not need to be refined. The issue now is how to offset the projected dark channel with a minimum filter of 1 degree. In this article, to do the compensation, an adaptive scaling factor is implemented. Halo and high computational cost issues are anticipated to be alleviated at the same moment.

More findings show that halos are predominantly around the abrupt grayscale shift region. We name this region Transmission Mis-estimated Region (TMR) where the

patch-wise transmission is mis-estimated. Pixel-wise and patch-wise designs therefore have their advantages and disadvantages. An optimization compromise between them is desirable. We suggest a fusion model for this purpose that combines pixel-wise dehazing models.

2.4 Calculation of PSNR, MSE and SSIM:

Mean Square Error (MSE) and Peak Signal to Noise Ratio (PSNR) are the two error metrics used to compare the quality of image compression. The MSE reflects the cumulative square error between the compressed and the initial picture, while PSNR is a maximum error metric. The smaller the MSE value, the lower the mistake.

- To compute the PSNR, the block first calculates the mean-squared error using the following equation:

$$MSE = \frac{\sum_{M,N} [I_1(m,n) - I_2(m,n)]^2}{M * N} \quad (2)$$

- In the previous equation, M and N are the number of rows and columns in the input images, respectively. Then the block computes the PSNR using the following equation:

$$PSNR = 10 \log_{10}(R^2 / MSE) \quad (3)$$

- In the previous equation, R is the maximum fluctuation in the input image data type. For example, if the input image has a double-precision floating-point data type, then R is 1. If it has an 8-bit unsigned integer data type, R is 255, etc.

The PSNR value should therefore be as large as possible in order to improve the effectiveness of the picture and the mean square error should be as small as possible. Therefore, for remote sensing pictures, it requires more iterations, generally more than 5 iterations, and is therefore known as Iterative dehazing. Compress the TMR in such a way that $M(tic)$ doesn't matter. $M(tic)$ slowly descends through the entire iteration. In the patch-wise transmission map, TMRs are almost non-existent. Since the IDeRS can suppress the halo artifacts dramatically, it offers amazingly excellent dehazing outcomes with rich data about the hue and clear details beyond other techniques. They are not adequate in processing information as well as saturation contrast when observing the dehazed pictures of GDCP and DHNet. CAP and NLD findings are somewhat over-saturated. Even though the methods of the BCCR and MS-CNN show good performance on the homogeneous hazy scenes, they are less robust to the heterogeneous hazy image.

3. Results:



Figure 4: Obtained output image-1, with the removal of haze and fog.

The PSNR for the image-1 is obtained as 28.07dB and SSIM as 0.9980 which is better than the previous techniques.



Figure 5: Obtained output image-2, with the removal of haze and fog.

The PSNR for the image-2 is obtained as 26.88 dB and SSIM as 0.9969 which is better than previous techniques.

Image	PSNR	SSIM	MSE
Image-1	28.07dB	0.9980dB	-0.86
Image-2	26.88dB	0.9969dB	-1.05

Table 3: Measurement of PSNR, SSIM and MSE of the obtained images.

4. Conclusion:

To conclude, the proposed network is able to remove moiré artefacts and haze pattern within every frequency band thanks to the non-linear multiresolution analysis of the moiré photos. People use their mobile phones to capture the content on screens for many reasons, such as convenience, simplicity, and efficiency. The large-scale benchmark together provides a decent solution to the hazy images and moire photo restoration with the increased PSNR and SSIM.

5. References:

[1] J. Beveridge *et al.*, "The challenge of face recognition from digital pointand- shoot cameras," in *Proc. IEEE Conf. Biometrics Theory, Appl. Syst.*, Oct. 2013, pp. 1-8.

[2] L. Wolf, T. Hassner, and I. Maoz, "Face recognition in unconstrained videos with matched background

similarity," in *Proc. IEEE Conf. Comput. Vis. Pattern Recognit.*, Jun. 2011, pp. 529-534.

[3] Z. Cui, W. Li, D. Xu, S. Shan, and X. Chen, "Fusing robust face region descriptors via multiple metric learning for face recognition in the wild," in *Proc. IEEE Conf. Comput. Vis. Pattern Recognit.*, Jun. 2013, pp. 3554-3561.

[4] L. Wolf and N. Levy, "The SVM-minus similarity score for video face recognition," in *Proc. IEEE Conf. Comput. Vis. Pattern Recognit.*, Jun. 2013, pp. 3523-3530.

[5] Y. Taigman, M. Yang, M. Ranzato, and L. Wolf, "Deep Face: Closing the gap to human-level performance in face verification," in *Proc. IEEE Conf. Comput. Vis. Pattern Recognit.* Jun. 2014, pp. 1701-1708.

[6] J. Hu, J. Lu, and Y. Tan, "Discriminative deep metric learning for face verification in the wild," in *Proc. IEEE Conf. Comput. Vis. Pattern Recognit.*, Jun. 2014, pp. 1875-1882.

[7] H. S. Bhatt, R. Singh, and M. Vatsa, "On recognizing faces in videos using clustering- based re-ranking and fusion," *IEEE Trans. Inf.*

[8] K. He, J. Sun, X. Tang, "Single image haze removal using dark channel prior," *IEEE Trans. Pattern Anal. Mach. Intell.* Vol. 33, Issue 12, pp. 1956-1963, 2011.

[9] C.-H. Hsieh, Y.-S. Lin, C.-H. Chang, "Haze removal without transmission map refinement based on dual dark channels," *International Conference on Machine Learning and Cybernetics*, 2014.

[10] R. Fattal, "Single image dehazing," *ACM Transactions on Graphics*, Vol. 27, No. 3, pp. 721-729, 2008.

[11] R. Tan "Visibility in bad weather from a single image," *IEEE Conference on Computer Vision and Pattern Recognition*, pp. 2347-2354, 2008.

[12] J.-H. Kim, W.-D. Jang, J.-Y. Sim, C.-S. Kim, "Optimized contrast enhancement for real-time image and video dehazing," *Journal of Visual Communication and Image Representation*, Vol. 24, Issue 3, pp. 410-425, February, 2013.

[13] Y.-H. Shiao, P.-Y. Chen, H.-Y. Yang, C.-H. Chen, and S.-S. Wang, "Weighted haze removal method with halo prevention," *Journal of Visual Communication and Image Representation*, Vol. 25, Issue 2, pp. 445-453, 2014.